












Article

Uranium Isotope Characterization in Volcanic Deposits in a High Natural Background Radiation Area, Mamuju, Indonesia

Ilsa Rosianna^{1,2}, Eka Djatnika Nugraha^{3,4,*}, Hirofumi Tazoe⁴, Heri Syaeful¹, Adi Gunawan Muhammad¹, I Gde Sukadana¹, Frederikus Dian Indrastomo¹, Ngadenin¹, Fadiyah Pratiwi¹, Agus Sumaryanto¹, Sucipta¹, Hendra Adhi Pratama¹, Deni Mustika¹, Leli Nirwani³, Nurokhim³, Yasutaka Omori^{3,4}, Masahiro Hosoda^{2,4}, Naofumi Akata⁴ and Shinji Tokonami⁴

- ¹ Research Center for Nuclear Fuel Cycle and Radioactive Waste Technology, Research Organization for Nuclear Energy, National Research and Innovation Agency (BRIN), South Tangerang 10340, Banten, Indonesia; ilsa001@brin.go.id (I.R.); heri021@brin.go.id (H.S.); adig001@brin.go.id (A.G.M.); igde001@brin.go.id (I.G.S.); fred002@brin.go.id (F.D.I.); ngad001@brin.go.id (N.); fadi005@brin.go.id (F.P.); agus029@brin.go.id (A.S.); suci002@brin.go.id (S.); hend031@brin.go.id (H.A.P.); deni010@brin.go.id (D.M.)
- ² Department of Radiation Science, Graduate School of Health Sciences, Hirosaki University, 66-1 Hon-cho, Hirosaki 036-8564, Aomori, Japan; m_hosoda@hirosaki-u.ac.jp
- ³ Research Center for Safety, Metrology, and Nuclear Technology, National Research and Innovation Agency (BRIN), South Tangerang 10340, Banten, Indonesia; leli001@brin.go.id (L.N.); nuro003@brin.go.id (N.); ys-omori@hirosaki-u.ac.jp (Y.O.)
- ⁴ Institute of Radiation Emergency Medicine, Hirosaki University, 66-1 Hon-cho, Hirosaki 036-8564, Aomori, Japan; tazoe@hirosaki-u.ac.jp (H.T.); akata@hirosaki-u.ac.jp (N.A.); tokonami@hirosaki-u.ac.jp (S.T.)
- * Correspondence: ekad001@brin.go.id



Citation: Rosianna, I.; Nugraha, E.D.; Tazoe, H.; Syaeful, H.; Muhammad, A.G.; Sukadana, I.G.; Indrastomo, F.D.; Ngadenin; Pratiwi, F.; Sumaryanto, A.; et al. Uranium Isotope Characterization in Volcanic Deposits in a High Natural Background Radiation Area, Mamuju, Indonesia. *Geosciences* **2023**, *13*, 388. <https://doi.org/10.3390/geosciences13120388>

Academic Editors: Micol Bussolesi and Jesus Martinez-Frias

Received: 17 November 2023

Revised: 9 December 2023

Accepted: 15 December 2023

Published: 17 December 2023



Copyright: © 2023 by the authors. Licensee MDPI, Basel, Switzerland. This article is an open access article distributed under the terms and conditions of the Creative Commons Attribution (CC BY) license (<https://creativecommons.org/licenses/by/4.0/>).

Abstract: Mamuju is an area of high natural radiation in Indonesia with high natural radiation levels (average 613 nSv h⁻¹). Mamuju is anomalous due to its high average ²³⁸U and ²³²Th concentrations of 22,882 and 33,549 Bq kg⁻¹, respectively, in laterite and rock. High natural radionuclide concentrations of ²³⁸U, ²³²Th, and ⁴⁰K have also been reported in soil samples from several locations in Mamuju, including Botteng, Northern Botteng, Takandeang, Ahu, and Taan. High radiation levels are related to radioactive mineral occurrences in the Adang volcanic complex, comprised of phonolitoid and foiditoid lithologies. According to the International Atomic Energy Agency (IAEA), uranium deposits can be classified into several types, among them a volcanic-related deposits, which include three sub-types: stratabound, structure-bound, and volcano-sedimentary deposits. This study aims to characterize volcanic rock deposit sub-types in the Mamuju area based on uranium radioisotope measurements. The uranium isotopes were measured using a tandem quadrupole inductively coupled plasma mass spectrometer combined with chemical separation by extraction chromatography using UTEVA resin. The analytical results for the ²³⁴U/²³⁸U ratios are used to determine the formation characteristics of minerals in each deposit sub-type based on mineral formation age, post-formation processes, and disturbances that affected the formation processes. Based on geochronological calculations using ²³⁴U/²³⁸U mineralization age, the deposits in the Mamuju area are 0.914–1.11 million years old and are classified as recent mineralization. These data have important implications for tracing uranium source rocks in the Mamuju area and may explain the anomalously high radiation levels in the Mamuju area.

Keywords: Mamuju; uranium disequilibrium analysis; geochemistry; extraction chromatography

1. Introduction

Mamuju is an area of Indonesia with high natural radiation levels (613 nSv h⁻¹) and represents a potential exploration area for radioactive minerals. Mamuju has anomalously high ²³⁸U and ²³²Th concentrations of 539–128,699 Bq kg⁻¹ (average: 22,882 Bq kg⁻¹)

and 471–288,639 Bq kg⁻¹ (average: 33,549 Bq kg⁻¹), respectively, in laterite and rock samples [1–3]. The geology of the Mamuju area is dominated by the Adang volcanic rock complex, which was formed by volcanic processes within the eruption center and several lava domes [4–6]. The formation of rocks within this volcanic complex is also associated with radioactive minerals in basaltic–andesitic lithologies [1,4,7].

In detail, the volcano stratigraphy of the Adang volcanic complex is divided into several small volcanoes (Ampalas, Mamuju, Takandeang, Sumare, and Tapalang; Figure 1). The Adang volcanic complex comprises peralkaline, peraluminous, and metaluminous rocks that are silica undersaturated [8]. Geochronology analysis using the potassium–argon (K–Ar) method indicates ages of 4.11 ± 0.1–2.75 ± 0.3 Ma for the Adang volcanic complex [5,8]. The lithology of the Adang volcanic complex is distinguished into several volcanic units, including phonolitoid and foiditoid lavas and volcanic breccia (autobreccia) units of the Ampalas, Mamuju, Takandeang, Sumare, and Tapalang volcanoes. These rocks have a hypocrySTALLINE texture, are porphyro-aphanitic, massive, and contain dominantly leucite and minerals including clinopyroxene, biotite, sanidine, orthoclase, plagioclase, apatite, hornblende, epidote, and opaque minerals.

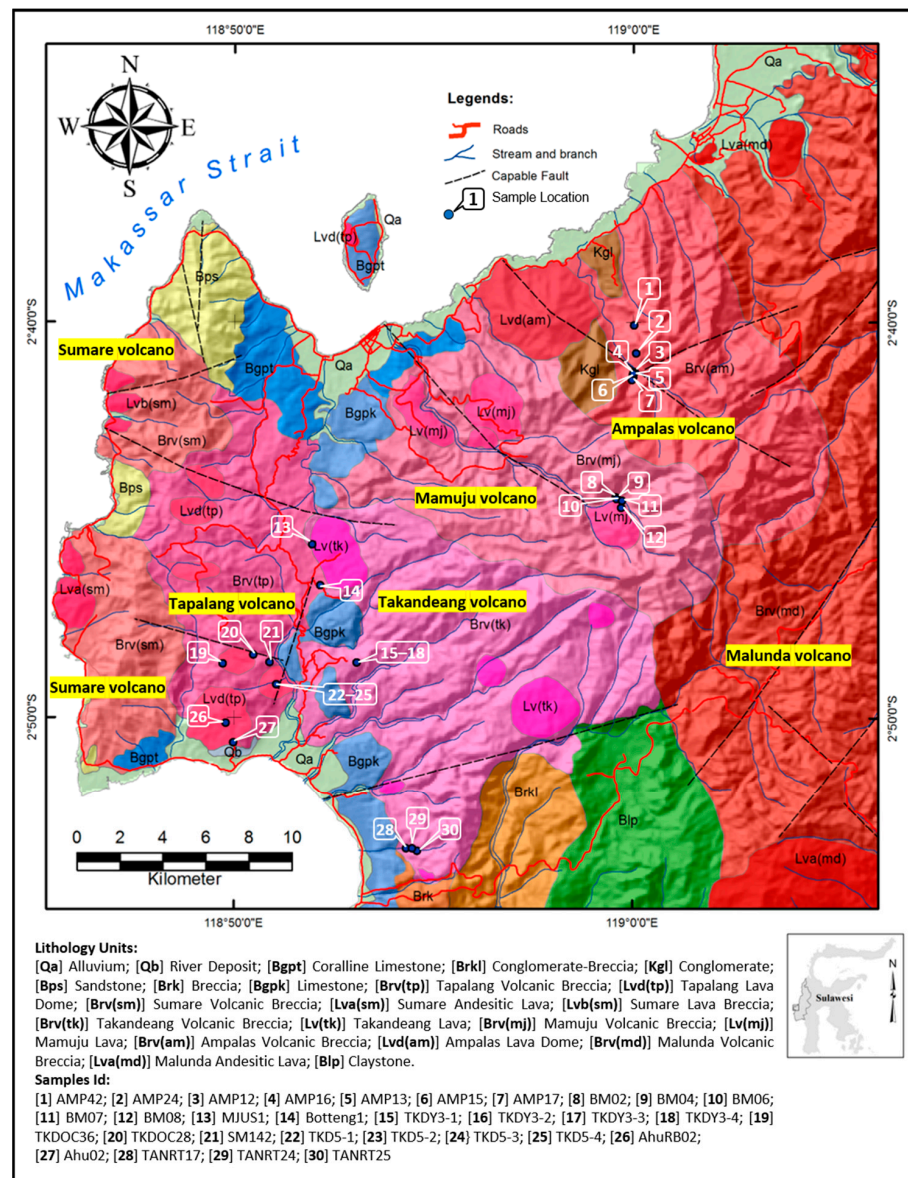


Figure 1. Geological map and sample locations in the vicinity of Mamuju, Indonesia (modified from [5,6,8]).

High uranium and thorium concentrations are recorded in weathered volcanic rocks in this area. The areas with high radiation dose rates in Mamuju are highly consistent with the distribution of the Adang volcanic deposits [2,4–6,9–12]. Some uranium and thorium minerals in this region are found in the form of davidite ((U,Ce,Fe)₂(Ti,Fe,V,Cr)₅O₁₂), thorianite (Th₂O), gummite (UO₃.nH₂O), autunite (CaO.2UO₃.P₂O₅.8H₂O) [13], britholite ((Ce,Ca)₅(SiO₄)₃OH), aeschynite (Ce,Ca,Fe,Th)(Ti,Nb)₂(O,OH)₆, monazite (REE,ThPO₄), thorite (ThSiO₄), and thorutite (Th,U,Ca)Ti₂(O,OH)₆ [14]. The enrichment process of the radioactive element (uranium and thorium) during fractional crystallization of Adang volcanic rocks is indicated by the increase in uranium and thorium levels in the rock. The positive correlation of alkaline content (K₂O + Na₂O + CaO) with the uranium and thorium elements is evidence of the association between radioactive elements and alkaline content. In the case of the three elements (K₂O + Na₂O + CaO), the enrichment from the beginning until the last phase increases by almost one order of magnitude. At low concentrations, thorium shows little scattering, whereas the plot of total alkaline element content (K₂O + Na₂O + CaO) vs. uranium shows a linear correlation [8].

According to the International Atomic Energy Agency (IAEA), most uranium deposits can be classified into sub-types (Table 1). Volcanic-related uranium deposits are associated with felsic to intermediate volcanic rocks and consist of three sub-types: stratabound, structure-bound, and volcano-sedimentary deposits [15]. Stratabound deposits occur in lava, autobreccias, tuff, and other rocks including welded tuff, vitrophyre, lapilli tuff, and ignimbrite. The mineralization in these deposit types is generally polymetallic, where uranium is associated with molybdenum and fluorine. These deposits are typically medium to large in scale (1000–40,000 tU) with moderate uranium concentrations (0.10–0.40% U) [15]. In contrast, structure-bound deposits form dispersed accumulations in permeable and chemically reactive streams, flow breccias, tuffs, and pyroclastic sediments. Globally, these deposits tend to be small to medium in size (500–5000 tU), with low to moderate uranium concentrations (0.03–0.10% U) [15,16]. In addition to these sub-types, volcano-sedimentary deposits consist of carbonaceous lacustrine or fluvial/alluvial sediments with a tuffaceous component. These deposits are widespread, peneconcordant, low-grade (50–200 ppm U) uranium accumulations associated with anomalous V, Mo, Li, F, B, Cu, and Ni content [15]. A schematic illustration of volcanic deposit mineralization is shown in Figure 2.

Table 1. Uranium volcanic-related deposits classification [15].

Type of Deposit	Sub-Type	Number of Deposits	U (t)
Volcanic-related	Stratabound	18	35,462
	Structure bound	86	552,161
	Volcano sedimentary	16	40,919

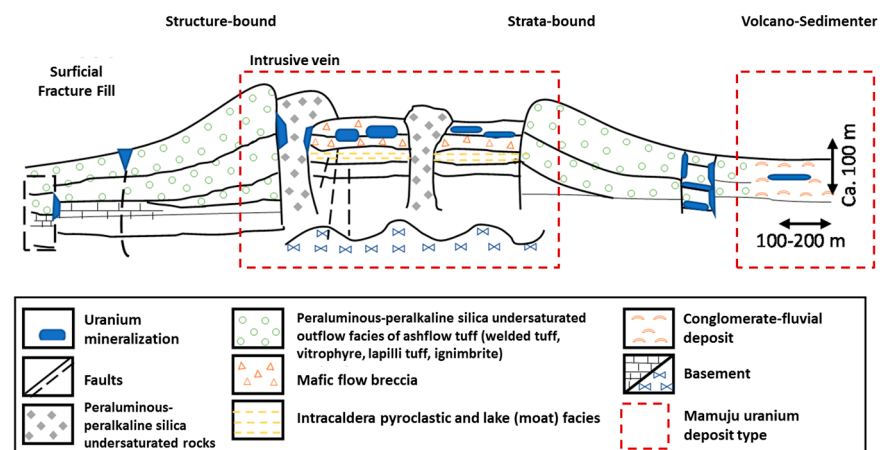


Figure 2. Schematic illustration for uranium deposit types from volcanic process (modified from [8,15]).

Hydrothermal and diagenetic processes can also affect the availability of uranium in volcanic deposits. As a mobile element, uranium will dissolve, leaving residual thorium as an immobile element; this results in supergene enrichment of immobile elements and the lateritization of mobile elements. Thus, uranium in volcanic rocks that undergo weathering and mineral accumulation on the surface (i.e., surface enrichment) will tend to form surficial deposits [17].

Uranium isotope ratio ($^{234}\text{U}/^{238}\text{U}$) analysis can be used to estimate the formation of minerals in each deposit sub-type depending on when the minerals were formed, post-formation processes, and the disturbances that have affected these processes. Accordingly, the present study uses disequilibrium analysis of uranium isotopes to characterize uranium deposit types in the Mamuju area. This work represents the first study to perform an isotopic characterization of the uranium deposits in the Mamuju area in Indonesia. The results of this study have important implications for tracing uranium source rocks in Mamuju and may explain the area's anomalously high radiation levels.

2. Materials and Methods

A total of 30 fresh samples were obtained from several subdistricts of the Mamuju area: Hulu Mamuju, Hulu Ampalas, Botteng, Takandeang, Rantedunia, Salumati Ahu, and Taan. These samples were the same as those described in previous research [1] (Figure 1). The purpose of collecting fresh rock is to avoid the influence of weathering factors that might affect the analysis of the samples.

2.1. Sampling and Preparation

Rock and soil samples were collected in locations with high radiation exposure and U-Th concentrations. The sample locations were selected based on radiation exposure using a NaI(Tl) scintillation detector. At these locations, a rock core drill was performed, and the outcrop was then observed using a magnifying glass and ultraviolet flashlight. After uranium was identified in the outcrop, further sampling was conducted at that location, and the coordinates of the site, the depth of rock or soil, and the rock or soil type at the site were recorded.

The rock/soil samples were dried using natural light for three days and then dried in an oven at 105 °C for 24 h. The dried samples were reduced to gravel grade with a hammer and subsequently milled and sieved to a size of 200 mesh. The samples were then heated at 400 °C using a furnace to remove organic material.

2.2. Pre-Concentration of Uranium and Thorium Using Extraction Chromatography

A mass of 50 g of each dried sample sieved to a size of 200 mesh was weighed. Several reference materials such as IAEA-357 (IAEA, Vienna, Austria), OREAS-124 (Mantra Resources Nyota Prospect, Lindi, Tanzania), and OREAS-465 (Tanzania-Mantra Resources Nyota Prospect) were put into microwave digestion (Ethos One, Palermo, Italy). The dissolution was performed three times with two concentration variations, namely 6 mL HNO_3 , 2 mL HCl , 1 mL HF , and 1 mL HClO_4 at 800 W with a temperature of 180 °C for one hour, then the temperature was increased to 200 °C for 20 min. The sample was subsequently evaporated on a hot plate. Furthermore, 4 mL 50% *v/v* HNO_3 was added to the sample and dried twice. Next, 4 mL of 25% *v/v* HNO_3 was added to the sample and dried. Finally, the sample was dissolved with up to 25 mL of 3M HNO_3 , at which stage it was ready for ICP-MS analysis [18,19]. Uranium isolation was performed using uranium tetravalent (UTEVA) resin (Eichrom, Lisle, USA) [20]. The resin was first rinsed with 5 mL of 3 M HNO_3 solution. The dissolved sample flowed through the resin column at 1 mL per minute. At the same flow rate, 5 mL of 9 M HCl and a mixture of 20 mL of 5 M HCl and 0.05 M oxalic acid flowed through the column. The uranium, assumed to be retained in the resin, was removed by flowing up to 15 mL of HCl 0.5 M through the column. The elution results were then collected in a container, and the eluted sample was dried on a hot plate.

A total of 10 mL of 3% HNO₃ *w/w* was added to the dry, which was then ready for ICP-MS analysis [21].

The total activity of ²³⁴U consists of components that are supported by secular equilibrium (and are equal to activity ²³⁸U) with Equations (1) and (2) as follows:

$$A(^{234}\text{U}) = A(^{238}\text{U}) + A(^{234}\text{U})_0 e^{-\lambda_{234}t} \quad (1)$$

$$A(^{234}\text{U}) = A(^{238}\text{U}) + [A(^{234}\text{U})_0 - A(^{238}\text{U})] e^{-\lambda_{234}t} \quad (2)$$

t to approximately 1 Ma with the Equation (3)

$$\frac{A(^{234}\text{U})}{A(^{238}\text{U})} = 1 + [\gamma_0 - 1] e^{-\lambda_{234}t} \quad (3)$$

where $A(^{234}\text{U})_0$ is the initial concentration of ²³⁴U, $A(^{234}\text{U})$ is the activity of ²³⁴U, $A(^{238}\text{U})$ is activity of ²³⁸U, λ_{234} is half life of ²³⁴U $2,8234 \times 10^{-6}$ year⁻¹, and γ_0 is initial concentration constant of ²³⁴U [22].

3. Results

Uranium mineralizations in the Mamuju area are related to the activities of volcano formation in the Adang volcanic complex [5,8]. Enrichment of radioactive elements happens due to recurrent magmatism processes with the development of alkaline magma into potassic, sodic, and calcic magmas [8]. Radioactive elements have been distinguished in accessory minerals and distributed, disseminated (stratabound), or developed in veinlets (structure-bound) in response to tectonic conditions in the area. In addition to stratabound and structure-bound, uranium mineralization is developed in laterite soil and volcano sedimentary [8]. Furthermore, where a multi-process occurs, that causes the radioactive elements to form an economic deposit. These deposits correlate with the volcanic-related deposits in the IAEA uranium deposit classification.

The stratabound deposit occurs in lava and autobreccia bodies of Adang volcanic complex. The deposit is distributed widely in the Ampalas, Takandeang, and Tapalang volcanoes. Phonolitoid and foiditoid lithologies characterize this deposit. Radioactive minerals identified in the area are davidite and thorianite as primary minerals and gummite and autunite as secondary minerals [13]. There are 24 samples analyzed, which present the stratabound deposit. Uranium isotope ratios vary in different geological rock units. The ratios show values from 0.77 to 1.3 (Table 2). Samples from Takandeang (samples 15 to 20) were collected from the lateritic soil layer in the area. This layer is a weathered phonolitoid rock that is formed near the surface. Since this layer has no uranium enrichment, these lateritic soils are grouped into stratabound deposit sub-types.

The structure-bound deposit is related to open space filling by fluids of magmatic origin. This deposit is identified in Hulu Mamuju, the central part of the research area. Hulu Mamuju is characterized by phonolitoid lava and autobreccia of the Mamuju volcano. Monazite, thorutite, and britholite are primary uranium in the vein [14] distributed in Mamuju lava. The uranium isotope ratios, measured from samples BM02 to BM08, range from 0.93 to 0.98 (Table 2).

In addition, the sample from Botteng area (Botteng1) is considered volcanic sedimentary. This sample is a conglomerate, a fluvial deposit of volcanic material. Gummite and autunite, the uranium secondary minerals, are identified in this deposit. The uranium isotope ratio is 0.75.

Table 2. Uranium isotope ratios from the samples in Adang volcanic complex.

No	Sample Id	$^{234}\text{U}/^{238}\text{U}$	Deposit	No	Sample Id	$^{234}\text{U}/^{238}\text{U}$	Deposit
1	AMP42	0.77	Stratabound	16	TKDY3-2	1.01	Stratabound
2	AMP24	0.98	Stratabound	17	TKDY3-3	0.96	Stratabound
3	AMP12	0.98	Stratabound	18	TKDY3-4	0.92	Stratabound
4	AMP16	1.08	Stratabound	19	TKDOC36	0.99	Stratabound
5	AMP13	1.12	Stratabound	20	TKDOC28	1.19	Stratabound
6	AMP15	0.89	Stratabound	21	SM142	0.73	Stratabound
7	AMP17	1.3	Stratabound	22	TKD5-1	0.95	Stratabound
8	BM02	0.97	Structure bound	23	TKD5-2	0.95	Stratabound
9	BM04	0.94	Structure bound	24	TKD5-3	0.9	Stratabound
10	BM06	0.98	Structure bound	25	TKD5-4	1	Stratabound
11	BM07	0.93	Structure bound	26	AhuRB02	1	Stratabound
12	BM08	0.98	Structure bound	27	Ahu02	0.92	Stratabound
13	MJUS1	1	Stratabound	28	TANRT17	1.25	Stratabound
14	Botteng1	0.75	Volcanic sedimenter	29	TANRT24	0.96	Stratabound
15	TKDY3-1	0.97	Stratabound	30	TANRT25	1.23	Stratabound

4. Discussion

Uranium can occur in various phases in various ligands. The combination of crystal size, valence, and crystal geometry dramatically influences the behavior of natural uranium minerals. The diversity of uranium minerals is also influenced by the evolution of the Earth over time due to the oxidation processes of rocks. There are two valence types of uranium minerals: hexavalent uranium and tetravalent uranium. Hexavalent uranium (^{234}U) is more easily mobilized than tetravalent uranium (^{238}U); thus, the mobilized hexavalent uranium undergoes a re-precipitation process when it interacts with reducing agents such as sulfides or certain minerals. Accordingly, the rock or mineral containing uranium undergoes structural damage or metamictization in which the daughter radionuclides are usually not captured in the parent lattice but instead migrate inside or outside the mineral [23]. Theoretically, in a closed system, ^{238}U and ^{234}U will be balanced or $^{234}\text{U}/^{238}\text{U} = 1$ [24]. The equilibrium measurement range assumed in this study is 0.95–1.05 to account for the uncertainty of the analysis process [25]. Some conditions that cause $^{234}\text{U}/^{238}\text{U} > 1$ occur due to an excess of ^{234}U , which is soluble and mobilized by water flow. In addition, the alpha recoil process causes ^{234}U to be thrown several μm from the rock core due to the “kickback” process from its parent, ^{234}Th , which has sufficient energy to shift the position of its whole progeny [26].

The ^{234}U mobilization by water increases the $^{234}\text{U}/^{238}\text{U}$ ratio (up to 12% ^{234}U), which can cause disequilibrium uranium isotopes [27]. This process spreads the uranium and causes changes in ion adsorption in minerals in the rock in its path. Due to the valence change from U (IV) to the more reactive U (VI), oxidation of metal elements in the surrounding rock or soil may occur. The ratio measurements of $^{234}\text{U}/^{238}\text{U}$ in the samples from the Mamuju area yielded a range of 0.73 to 1.30. Assuming secular equilibrium, the ratio of the parent’s activity to the offspring’s equilibrium is 1 [24,25,28]. Activity ratio values of $^{234}\text{U}/^{238}\text{U} > 1$ occur because of excess amounts of ^{234}U in the sample. In contrast, if $^{234}\text{U}/^{238}\text{U} < 1$, the sample is unbalanced or still recent [28,29]. Samples with an activity ratio of $^{234}\text{U}/^{238}\text{U} = 1$ are in equilibrium. The summary of the characteristics of uranium isotopes in volcanic-deposit types of Mamuju samples is shown in Table 3.

Table 3. Characteristics of uranium isotopes in the volcanic-deposit type from the Mamuju area.

Sample	$^{234}\text{U}/^{238}\text{U}$	Classification	Deposit of Control	Type of Rock Texture	Rock Unit
BM02	0.97	equilibrium	structure bound	lava phonolitoid	Lava Mamuju
BM04	0.94	disequilibrium	structure bound	lava phonolitoid	Lava Mamuju
BM06	0.98	equilibrium	structure bound	lava phonolitoid	Lava Mamuju
BM07	0.93	disequilibrium	structure bound	lava phonolitoid	Lava Mamuju
BM08	0.98	equilibrium	structure bound	lava phonolitoid	Lava Mamuju
MJUS1	1	equilibrium	stratabound	soil	Lava takandeang
TANRT24	0.96	equilibrium	stratabound	lava phonolitoid	Takandeang volcanic breccia
TANRT17	1.25	remobilization of uranium	stratabound	lava phonolitoid autobreccia	Takandeang volcanic breccia
TANRT25	1.23	remobilization of uranium	stratabound	lava phonolitoid	Takandeang volcanic breccia
TKD5-1	0.95	equilibrium	stratabound	lava phonolitoid autobreccia	Tapalang lava dome
TKD5-2	0.95	equilibrium	stratabound	lava phonolitoid autobreccia	Tapalang lava dome
TKD5-3	0.9	disequilibrium	stratabound	lava phonolitoid autobreccia	Tapalang lava dome
TKD5-4	1	equilibrium	stratabound	lava phonolitoid autobreccia	Tapalang lava dome
AMP17	1.3	remobilization of uranium	stratabound	lava foiditoid	Ampalas volcanic breccia
AhuRB02	1	equilibrium	stratabound	lava phonolitoid pillow lava	Tapalang lava dome
Ahu02	0.92	disequilibrium	stratabound	lava foiditoid	Tapalang lava dome
AMP12	0.98	equilibrium	stratabound	lava foiditoid	Ampalas volcanic breccia
SM142	0.73	disequilibrium	stratabound	lava foiditoid	Tapalang volcanic breccia
AMP13	1.12	remobilization of uranium	stratabound	lava foiditoid	Ampalas volcanic breccia
AMP15	0.89	disequilibrium	stratabound	lava foiditoid	Ampalas volcanic breccia
AMP42	0.77	disequilibrium	stratabound	lava foiditoid	Ampalas volcanic breccia
AMP24	0.98	equilibrium	stratabound	lava foiditoid	Ampalas volcanic breccia
AMP16	1.08	remobilization of uranium	stratabound	lava foiditoid	Ampalas volcanic breccia
TKDOC28	1.19	remobilization of uranium	laterite	lava phonolitoid	Tapalang lava dome
TKDOC36	0.99	equilibrium	laterite	lava phonolitoid	Tapalang volcanic breccia
TKDY3-1	0.97	equilibrium	laterite	weathered phonolitoid	Takandeang volcanic breccia
TKDY3-2	1.01	equilibrium	laterite	weathered phonolitoid	Takandeang volcanic breccia
TKDY3-3	0.96	equilibrium	laterite	weathered phonolitoid	Takandeang volcanic breccia
TKDY3-4	0.92	disequilibrium	laterite	weathered phonolitoid	Takandeang volcanic breccia
Botteng1	0.75	disequilibrium	volcano sedimentary	conglomerate	Tapalang volcanic breccia

In theory, the stratabound deposit sub-type represents overlapping layers of bedded lava and thus has lower porosity and permeability than the structure-bound sub-type, reducing the tendency of the samples to be disturbed. In the stratabound deposit, several isotope ratios were identified with $^{234}\text{U}/^{238}\text{U} > 1$. These samples are collected from

the Takandeang volcanic breccia unit (TANRT17 and TANRT25) and the Ampalas volcanic breccia unit (AMP13, AMP16, and AMP17). The Takandeang volcanic breccia unit comprises phonolitoid rocks, while the Ampalas volcanic breccia unit is foiditoid rocks. Foiditoids and phonolitoids differ in their feldspathoid, plagioclase, and alkali-feldspar contents. Mineralogical characteristics of foiditoid rocks have more abundant and large leucite crystals than phonolitoid rocks. In these examples, compositional or formation process differences between successive lava flows may result in variations in the minerals formed in each layer. Differences in temperature and pressure also affect the formation of uranium crystal lattices. The lattice fields on the crystal significantly affect the behavior and properties of the material. Compositional differences in the formation of minerals will create a non-uniformity of crystal shapes that affect the crystal lattice so that water rapidly enters the ^{234}U and thus disturbs the system's equilibrium. Several natural processes can disrupt this equilibrium, such as chemical drying, precipitation from solution, and re-crystallization [30]. The precipitation from the solution might be a dominant factor in Ampalas samples (AMP13, AMP16, and AMP17). The steep morphology of the river made the flow of water isolated in the watershed. At some locations in the river, conditions in a reducing environment allow uranium to precipitate.

In addition, several samples had $^{234}\text{U}/^{238}\text{U}$ values close to 1, indicating that they were part of a closed system and reached secular equilibrium. These include outcrop samples located in the Takandeang lava unit (MJUS1), the Takandeang volcanic breccia unit (TANRT24), the Tapalang lava dome unit (AhuRB02), and the Ampalas volcanic breccia unit (AMP24, AMP12), and subsurface samples of Tapalang lava dome unit from the Takandeang drillhole at depths of 7.37–7.42 m (TKD5-1), 7.47–7.52 m (TKD5-4), and 7.82–7.87 m (TKD5-2). The other stratabound sub-type samples were classified as recent mineralization because they had not yet reached equilibrium, including those located in Tapalang lava dome surface units (Ahu02), Tapalang volcanic breccia units (SM142), Ampalas volcanic breccia units (AMP15 and AMP42), and subsurface Tapalang lava dome units from the Takandeang drillhole at a depth of 7.57–7.62 m (TKD5-3). The isotope ratio measurements for the stratabound deposit sub-type are shown in Table 4.

Table 4. Uranium isotope ratios in stratabound deposit sub-type on rock samples.

No	Sample	Type of Rock Texture	Rock Unit	$^{234}\text{U}/^{238}\text{U}$	Classification
1	AMP15	Foiditoid	Ampalas volcanic breccia	0.89	Disequilibrium
2	AMP42	Foiditoid	Ampalas volcanic breccia	0.77	Disequilibrium
3	AMP12	Foiditoid	Ampalas volcanic breccia	0.98	Equilibrium
4	AMP24	Foiditoid	Ampalas volcanic breccia	0.98	Equilibrium
5	AMP13	Foiditoid	Ampalas volcanic breccia	1.12	Remobilization of uranium
6	AMP16	Foiditoid	Ampalas volcanic breccia	1.08	Remobilization of uranium
7	AMP17	Foiditoid	Ampalas volcanic breccia	1.3	Remobilization of uranium
8	MJUS1	Soil	Takandeang lava	1	Equilibrium
9	TKD5-1	Phonolitoid	Tapalang lava dome	0.95	Equilibrium
10	TKD5-2	Phonolitoid	Tapalang lava dome	0.95	Equilibrium
11	TKD5-3	Phonolitoid	Tapalang lava dome	0.9	Disequilibrium
12	TKD5-4	Phonolitoid	Tapalang lava dome	1	Equilibrium
13	AhuRB02	Phonolitoid	Tapalang lava dome	1	Equilibrium
14	Ahu02	Foiditoid	Tapalang lava dome	0.92	Disequilibrium
15	SM142	Foiditoid	Tapalang volcanic breccia	0.73	Disequilibrium
16	TANRT24	Phonolitoid	Takandeang volcanic breccia	0.96	Equilibrium
17	TANRT17	Phonolitoid	Takandeang volcanic breccia	1.25	Remobilization of uranium
18	TANRT25	Phonolitoid	Takandeang volcanic breccia	1.23	Remobilization of uranium

Several laterite areas are identified in the stratabound sub-type area in Takandeang and Rantedunia (Table 5). These laterites are derived from weathering process of volcanic rocks (phonolitoid lava and autobreccia) on the surface due to chemical, physical, and biological

factors [13,31]. However, these laterites did not undergo uranium enrichment. The uranium in this location is not considered a surficial (laterite) deposit but is classified into volcanic-related types on stratabound sub-type deposits. The TKDOC28 and TKDOC36 were collected from the Tapalang lava dome unit, characterized by phonolitic lava. Meanwhile, samples TKDY3-1 to TKDY3-4 were recovered from the drillhole at a depth of 17 m, characterized by phonolitic autobreccia from the Takandeang volcanic breccia unit.

Table 5. Isotope ratios in stratabound sub-type deposit on laterite samples.

No	Sample	Type of Rock Texture	Rock Unit	²³⁴ U/ ²³⁸ U	Classification
1	TKDOC28	Phonolitic	Tapalang lava dome	1.19	Remobilization of Uranium
2	TKDOC36	Phonolitic	Tapalang lava dome	0.99	Equilibrium
3	TKDY3-2	Phonolitic	Takandeang volcanic breccia	1.01	Equilibrium
4	TKDY3-1	Phonolitic	Takandeang volcanic breccia	0.97	Equilibrium
5	TKDY3-3	Phonolitic	Takandeang volcanic breccia	0.96	Equilibrium
6	TKDY3-4	Phonolitic	Takandeang volcanic breccia	0.92	Disequilibrium

A ²³⁴U/²³⁸U isotope ratio value greater than 1 is recorded in a laterite sample from the Tapalang lava dome units (TKDOC28). In this sample, uranium accumulation is likely due to the weathering process. Equilibrium results are identified in the Tapalang volcanic breccia unit (TKDOC36) and drillhole in Rantedunia at depths of 17.29–17.34 m (TKDY3-2), 17.34–17.39 m (TKDY3-1), and 17.59–17.64 m (TKDY3-3), while the sample a depth of 17.84–17.89 m (TKDY3-4) is still in disequilibrium. The ²³⁴U/²³⁸U activity ratio relationship showed that ²³⁴U was dissolving from the soil, but there was no significant U disequilibrium between ²³⁴U and ²³⁸U. This could have been caused by the high ²³⁸U concentration and negligible ²³⁴U leaching, which may not have been significant enough to cause a change in the ²³⁴U/²³⁸U activity ratio. The high concentration of ²³⁸U and the small quantity of ²³⁴U leaching may be too modest to be reflected in the ²³⁴U/²³⁸U ratio [32]. The condition of equilibrium/disequilibrium in TKD samples is believed to reflect the previous state of the deposit before weathering.

Geological structures, like joints and faults, control uranium mineralization in the Mamuju upstream (Hulu Mamuju). In fractured rocks, the uranium ores appears as fissure and filling joints, directing N 240° E and N 300° E. The resulting structural elements filled by hydrothermal solutions containing mobile uranium elements, which ultimately form the structure-bound mineralization deposit. Samples from Hulu Mamuju, BM-02 to BM-08, were collected from the Mamuju lava rock unit. The ratio measurement results are <1 (Table 6), indicating several recent deposits. In this structure-bound sub-type, near-equilibrium to equilibrium conditions are recorded based on the uranium isotope ratios.

Table 6. Uranium isotope ratios in the structure-bound deposit sub-type on rock samples.

No	Sample	Type of Rock Texture	Rock Unit	²³⁴ U/ ²³⁸ U	Classification
1	BM02	Phonolitic	Mamuju lava	0.97	Equilibrium
2	BM04	Phonolitic	Mamuju lava	0.94	disequilibrium
3	BM06	Phonolitic	Mamuju lava	0.98	Equilibrium
4	BM07	Phonolitic	Mamuju lava	0.93	disequilibrium
5	BM08	Phonolitic	Mamuju lava	0.98	Equilibrium

The classification of the volcano-sedimentary deposit sub-type sample is listed in Table 7. This uranium deposit occurs in volcano-sedimentary rock re-deposited in a reducing environment. The isotope ratio for this conglomerate sample from the Tapalang volcanic breccia unit (Botteng1) has not yet reached equilibrium: it is characterized by an isotope ratio < 1 and classified as recent mineralization.

Table 7. Isotope ratio measurement in volcano-sedimentary deposit sub-type on rock sample.

No	Sample	Type of Rock Texture	Rock Unit	²³⁴ U/ ²³⁸ U	Classification
1	Botteng1	Conglomerate	Tapalang volcanic breccia	0.75	disequilibrium

Disequilibrium analysis of the ²³⁴U/²³⁸U isotope ratios can also be applied to calculate a sample’s mineralization age. This measurement uses the principle of calculating the radioactive decay of the isotopes ²³⁴U and ²³⁸U [22,25]. The mineralization age is crucial in constraining minerals’ formation and distribution and selecting the appropriate method for uranium mineral exploration. Based on the results of geochronological calculations using the ²³⁴U/²³⁸U series (Figure 3), the mineralization ages in Mamuju range from 0.914 to 1.11 Ma and are classified as recent mineralization. These values indicate that Mamuju uranium mineralization is Quaternary in period [15,22].

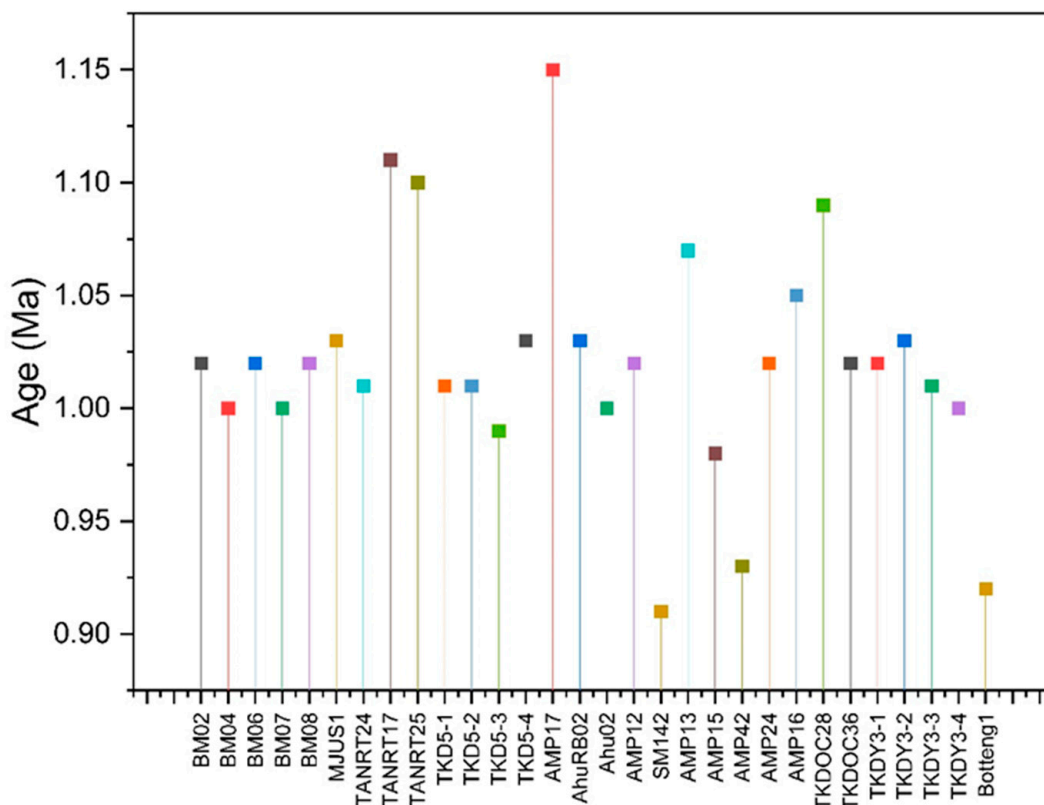


Figure 3. Recent age for uranium mineralized samples from the Mamuju area.

5. Conclusions

Mamuju is an anomalous area due to its high U and Th concentrations and has potential as an exploration area for radioactive minerals. In this study, the analytical results of the uranium isotope ratio ²³⁴U/²³⁸U were used to characterize the mineralization in each deposit sub-type based on the mineral formation age, post-formation processes, and disturbances that have affected formation processes in the stratabound, structure-bound, and volcano-sedimentary deposit types.

- Uranium mineralizations in stratabound deposits are in various equilibriums. The Takandeang volcanic breccia hosts stratabound deposits and most are at equilibrium. Oxidation and groundwater is the main factor of uranium remobilization. The weathering process has a less significant impact on uranium remobilization.

- The Mamuju lava hosts structure-bound deposits, in which uranium fills the fissures in lava due to faulting. Some of the uranium in structure-bound is disequilibrium, and some is equilibrium without further remobilization.
- The Ampal volcanic breccia hosts a stratabound deposit most at equilibrium. Some of the equilibrium uranium is further remobilized, interpreted as influenced by ground-water and the reduction–oxidation environment.
- The Tapalang lava dome hosts stratabound deposits, where some have undergone a weathering process into laterite. Most laterite samples show no remobilization process of uranium. Tapalang volcanic breccia hosts the stratabound and volcano-sedimentary deposits. Both deposits show a meager disequilibrium ratio.
- Based on geochronological calculations, the mineralization ages in the Adang volcanic complex range from 0.914 to 1.11 Ma and are classified as recent mineralization.
- These data provide essential constraints for tracing uranium source rocks in the Mamuju area and may explain the area’s anomalously high radiation exposure levels.

Author Contributions: Conceptualization, E.D.N. and S.T.; methodology, E.D.N., H.T., I.R., N.A., H.S., I.G.S., N. (Ngadenin), A.S., S. and Y.O.; validation, I.R., H.S., N. (Ngadenin), D.M., L.N., H.A.P., N. (Nurokhim), A.G.M., I.G.S. and E.D.N.; formal analysis, E.D.N. and I.R.; investigation, H.S., A.G.M., I.G.S., F.D.I., N. (Ngadenin), I.R., N. (Nurokhim), A.S., D.M., E.D.N. and S.; resources, E.D.N., I.R., A.S., Y.O., M.H., N.A. and S.T.; data curation, E.D.N., I.R., F.P., L.N., N. (Ngadenin) and F.D.I.; writing—original draft preparation, I.R. and E.D.N.; writing—review and editing, I.R., E.D.N., H.T., H.S., A.G.M., I.G.S., F.D.I., N. (Nurokhim), S., N. (Ngadenin), D.M., L.N., H.A.P., F.P., A.S., M.H., Y.O., N.A. and S.T.; visualization, E.D.N., F.D.I., I.R., H.S. and F.P.; supervision, E.D.N., H.S., N.A., I.G.S., N. (Ngadenin), A.S., S. and S.T.; funding acquisition, S.T., M.H., I.R., Y.O. and E.D.N. All authors have read and agreed to the published version of the manuscript.

Funding: The Japan Society partially supported this work for the Promotion of Science (JSPS) Environmental Radioactivity Network Center (ERAN) Grant No I-22–14 and I-23–34 (EDN, IR); The Japan Society for the Promotion of Science (JSPS) KAKENHI Grant nos. JP16K15368, JP16H02667, JP18KK0261, JP18K10023, JP20H00556 (ST, MH); Ministry of Research, Technology and Higher Education Indonesia and the Indonesia Endowment Funds for Education (LPDP) through the research fund Riset Inovasi untuk Indonesia Maju (RIIM) Grant No RIIM-16 (E.D.N) and National Nuclear Energy Agency (BATAN) through research fund Center for Nuclear Minerals Technology (PTBGN); The Management Talenta-BRIN through the visiting researcher program 2022 (E.D.N; and Y.O).

Institutional Review Board Statement: This study is not related to any ethical issues, such as research involving animals and the protection of human subjects.

Data Availability Statement: All relevant data are in this paper.

Acknowledgments: The authors acknowledge and are grateful to the author’s colleagues from the Mamuju exploration group and the local people for their help during the investigation in the study area. Moreover, our gratitude goes to Japan International Cooperation Agency (JICA) - SDGs Global Leader Scholarship programme that has funded the author at Hirosaki University (Awardee: Ilsa Rosianna).

Conflicts of Interest: The authors have no competing interest to declare that are relevant to the content of this article.

References

1. Rosianna, I.; Nugraha, E.D.; Syaeful, H.; Putra, S.; Hosoda, M.; Akata, N.; Tokonami, S. Natural radioactivity of laterite and volcanic rock sample for radioactive mineral exploration in Mamuju, Indonesia. *Geoscience* **2020**, *10*, 376. [[CrossRef](#)]
2. Nugraha, E.D.; Hosoda, M.; Tamakuma, Y.; Kranrod, C.; Mellawati, J.; Akata, N.; Tokonami, S. A unique high natural background radiation area in Indonesia: A brief review from the viewpoint of dose assessments. *J. Radioanal. Nucl. Chem.* **2021**, *330*, 1437–1444. [[CrossRef](#)]
3. Nugraha, E.D.; Mellawati, J.; Wahyudi; Kranrod, C.; Makhsum; Tazoe, H.; Ahmad, H.; Hosoda, M.; Akata, N.; Tokonami, S. Heavy metal assessments of soil samples from a high natural background radiation area, Indonesia. *Toxics* **2022**, *10*, 39. [[CrossRef](#)] [[PubMed](#)]
4. Syaeful, H.; Sukadana, I.G.; Sumaryanto, A.; Sumaryanto, A. Radiometric mapping for Naturally Occurring Radioactive Materials (NORM) assessment in Mamuju, West Sulawesi. *Atom Indones.* **2014**, *40*, 35. [[CrossRef](#)]

5. Sukadana, I.G.; Harijoko, A.; Setijadji, L.D. Tectonic setting of Adang volcanic complex in Mamuju Region, West Sulawesi Province. *Eksplorium* **2015**, *36*, 31–44. [[CrossRef](#)]
6. Indrastomo, F.D.; Sukadana, I.G.; Saepuloh, A.; Harsolumakso, A.H.; Kamajati, D. Volcanostratigraphy interpretation of Mamuju area based on Landsat-8 imagery analysis. *Eksplorium* **2015**, *36*, 71–88. [[CrossRef](#)]
7. Ratman, N.; Atmawinata, S. *Geological Map of the Mamuju Quadrangle, Sulawesi*; Pusat Penelitian dan Pengembangan Geologi: Bandung, Indonesia, 1993.
8. Sukadana, I.G. Magma Evolution and Radioactive Minerals Enrichment in Adang Volcanic Rocks in Mamuju, West Sulawesi. Doctoral Dissertation, Universitas Gadjah Mada, Sleman, Indonesia, 2023.
9. Sukadana, I.G.; Warmada, I.W.; Harijoko, A.; Indrastomo, F.D.; Syaeful, H. The application of geostatistical analysis on radiometric mapping data to recognized the uranium and thorium anomaly in West Sulawesi, Indonesia. *IOP Conf. Ser. Earth Environ. Sci.* **2021**, *819*. [[CrossRef](#)]
10. Mu'awanah, F.R.; Priadi, B.; Widodo, W.; Sukadana, I.G.; Andriansyah, R. Uranium mobility of active stream sediment in Mamuju area, West Sulawesi. *Eksplorium* **2019**, *39*, 95. [[CrossRef](#)]
11. Nugraha, E.D.; Hosoda, M.; Kusdiana; Winarni, I.D.; Prihantoro, A.; Suzuki, T.; Tamakuma, Y.; Akata, N.; Tokonami, S. Dose assessment of Radium-226 in drinking water from Mamuju, a high background radiation area of Indonesia. *Radiat. Environ. Med.* **2020**, *9*, 79–83.
12. Hosoda, M.; Nugraha, E.D.; Akata, N.; Yamada, R.; Tamakuma, Y.; Sasaki, M.; Kelleher, K.; Yoshinaga, S.; Suzuki, T.; Rattanapongs, C.P.; et al. A unique high natural background radiation area—Dose assessment and perspectives. *Sci. Total Environ.* **2021**, *750*, 142346. [[CrossRef](#)]
13. Sukadana, I.G.; Syaeful, H.; Indrastomo, F.D.; Widana, K.S.; Rakhma, E. Identification of mineralization type and specific radioactive minerals in Mamuju, West Sulawesi. *J. East China Univ. Technol.* **2016**, *39*, 39–48.
14. Sukadana, I.G.; Warmada, I.W.; Pratiwi, F.; Harijoko, A.; Adimedha, T.B. Elemental mapping for characterizing of thorium and Rare Earth Elements (REE) bearing minerals using μ XRF. *Atom Indones.* **2022**, *48*, 87–98. [[CrossRef](#)]
15. International Atomic Energy Agency. *Geological Classification of Uranium Deposits and Description of Selected Examples*; IAEA-TECDOC-1842; IAEA: Vienna, Austria, 2018.
16. Shin, W.; Oh, J.; Choung, S.; Cho, B.W.; Lee, K.S.; Yun, U.; Woo, N.C.; Kim, H.K. Distribution and potential health risk of groundwater uranium in Korea. *Chemosphere* **2016**, *163*, 108–115. [[CrossRef](#)] [[PubMed](#)]
17. Dahlkamp, F.J. *Uranium Ore Deposits*; Springer: Berlin/Heidelberg, Germany, 1993.
18. Liu, C.; Hu, B.; Shi, J.; Li, J.; Zhang, X.; Chen, H. Determination of uranium isotopic ratio ($^{235}\text{U}/^{238}\text{U}$) using extractive electrospray ionization tandem mass spectrometry. *J. Anal. At. Spectrom.* **2011**, *26*, 2045–2051. [[CrossRef](#)]
19. Oh, S.Y.; Lee, S.A.; Park, J.H.; Lee, M.; Song, K. Isotope measurement of uranium at ultratrace levels using multicollector inductively coupled plasma mass spectrometry. *Mass Spectrom. Lett.* **2012**, *3*, 54–57. [[CrossRef](#)]
20. Horwitz, E.P.; Dietz, M.L.; Chiarizia, R.; Diamond, H.; Essling, A.M.; Graczyk, D. Separation and preconcentration of uranium from acidic media by extraction chromatography. *Anal. Chim. Acta* **1992**, *266*, 25–37. [[CrossRef](#)]
21. Rosianna, I.; Syaeful, H.; Putra, S.; Rakhma, E.; de Sukadana, I.G.; Nugraha, E.D.; Tazoe, H.; Akata, N. A novel uranium measurement using extraction chromatography separation technique in radioactive minerals exploration. *AIP Conf. Proc.* **2022**, *2638*, 030002. [[CrossRef](#)]
22. Allègre, C.J. *Isotope Geology*; Cambridge University Press: Cambridge, UK, 2008; ISBN 9780521862288.
23. Cook, N.J.; Ehrig, K.J.; Rollog, M.; Ciobanu, C.L.; Lane, D.J.; Schmandt, D.S.; Owen, N.D.; Hamilton, T.; Grano, S.R. ^{210}Pb and ^{210}Po in Geological and Related Anthropogenic Materials: Implications for Their Mineralogical Distribution in Base Metal Ores. *Minerals* **2018**, *8*, 211. [[CrossRef](#)]
24. Fujikawa, Y.; Fukui, M.; Sasaki, T.; Kudo, A.; Sugahara, M.; Okano, Y.; Ikeda, E.; Yunoki, E.; Kataoka, H. Variation in uranium isotopic ratios U-234/U-238 and U-235/U-238 in Japanese soil and water samples. Application to environmental monitoring. In Proceedings of the International Congress of the International Radiation Protection Association, Hiroshima, Japan, 14–19 May 2000.
25. Pekala, M.; Kramers, J.D.; Waber, H.N. $^{234}\text{U}/^{238}\text{U}$ activity ratio disequilibrium technique for studying uranium mobility in the Opalinus Clay at Mont Terri, Switzerland. *Appl. Radiat. Isot.* **2010**, *68*, 984–992. [[CrossRef](#)]
26. Fantle, M.S.; Maher, K.M.; Depaolo, D.J. Isotopic approaches for quantifying the rates of marine burial diagenesis. *Rev. Geophys.* **2010**, *48*, 1–38. [[CrossRef](#)]
27. Andersen, M.B.; Elliott, T.; Freymuth, H.; Sims, K.W.W.; Niu, Y.; Kelley, K.A. The terrestrial uranium isotope cycle. *Nature* **2015**, *517*, 356–359. [[CrossRef](#)] [[PubMed](#)]
28. Bonotto, D.M.; Jiménez-Rueda, J.R.; Fagundes, I.C.; Filho, C.R.A.F. Weathering processes and dating of soil profiles from São Paulo State, Brazil, by U-isotopes disequilibria. *Appl. Radiat. Isot.* **2017**, *119*, 6–15. [[CrossRef](#)] [[PubMed](#)]
29. Handley, H.K.; Turner, S.P.; Dosseto, A.; Haberland, D.; Afonso, J.C. Considerations for U-series dating of sediments: Insights from the Flinders Ranges, South Australia. *Chem. Geol.* **2013**, *340*, 40–48. [[CrossRef](#)]
30. Keech, A.R.; West, A.J.; Pett-Ridge, J.C.; Henderson, G.M. Evaluating U-series tools for weathering rate and duration on a soil sequence of known ages. *Earth Planet. Sci. Lett.* **2013**, *374*, 24–35. [[CrossRef](#)]

31. Min, M.; Chen, J.; Wang, J.; Wei, G.; Fayek, M. Mineral paragenesis and textures associated with sandstone-hosted roll-front uranium deposits, NW China. *Ore Geol. Rev.* **2005**, *26*, 51–69. [[CrossRef](#)]
32. Veerasamy, N.; Kasar, S.; Murugan, R.; Inoue, K.; Natarajan, T.; Chand Ramola, R.; Fukushi, M.; Kumar Sahoo, S. $^{234}\text{U}/^{238}\text{U}$ disequilibrium and $^{235}\text{U}/^{238}\text{U}$ ratios measured using MC-ICP-MS in natural high background radiation area soils to understand the fate of uranium. *Chemosphere* **2023**, *323*, 138217. [[CrossRef](#)]

Disclaimer/Publisher's Note: The statements, opinions and data contained in all publications are solely those of the individual author(s) and contributor(s) and not of MDPI and/or the editor(s). MDPI and/or the editor(s) disclaim responsibility for any injury to people or property resulting from any ideas, methods, instructions or products referred to in the content.